Pharmaceutical Research, Vol. 8, No. 4, 1991

Research Article

Hepatic Disposition Characteristics of Electrically Charged Macromolecules in Rat *in Vivo* and in the Perfused Liver

Koyo Nishida,[1] Kiyoshi Mihara,[1] Toichi Takino,[1] Sachi Nakane,[1] Yoshinobu Takakura,[1] Mitsuru Hashida,[1] and Hitoshi Sezaki[1,2]

Received June 29, 1990; accepted November 20, 1990

The effect of electric charge on the hepatic disposition of macromolecules was studied in the rat. Charged derivatives of dextran (T-70) and bovine serum albumin (BSA), mitomycin C–dextran conjugates (MMC-D), and lactosaminated BSA (Lac-BSA) were employed as model macromolecules. After intravenous injection, cationic macromolecules were rapidly eliminated from plasma because of their extensive hepatic uptake, while anionic and neutral macromolecules were slowly eliminated. Cationic macromolecules were recovered from parenchymal and nonparenchymal hepatic cells at a cellular uptake (per unit cell number) ratio of 1.4–3.2, while that of Lac-BSA was 14. During liver perfusion using a single-pass constant infusion mode, cationic macromolecules were continuously extracted by the liver, with extraction ratios at steady-state (E_{ss}) ranging between 0.03 and 0.54, whereas anionic and neutral macromolecules were almost completely recovered in the outflow at steady state. The E_{ss} for cationized BSA (Cat-BSA) and cationic MMC-Dcat were concentration dependent and decreased at low temperatures and in the presence of colchicine and cytochalasin B. The possible participation of the internalization process in the uptake of cationic macromolecules by hepatocytes was suggested.

KEY WORDS: electric charge; model macromolecule; hepatic disposition; cellular localization; constant infusion; adsorptive endocytosis.

INTRODUCTION

Macromolecular carrier systems have been developed to achieve site-specific delivery or prolonged retention in the circulation of drugs such as antitumor agents and peptides (1–3). The conjugation of such compounds with macromolecules changes their *in vivo* disposition characteristics. However, the application of macromolecular carriers has been frequently limited by their hepatic uptake and degradation.

We have previously examined the pharmacokinetic characteristics of polymeric prodrugs of mitomycin C (MMC), which were mitomycin C–dextran conjugates (MMC-D) having cationic (MMC-Dcat) and anionic (MMC-Dan) charges (1,2). An *in vivo* disposition study in rats and mice demonstrated marked accumulation of MMC-Dcat in the liver, while MMC-Dan showed a low plasma clearance and little accumulation in the liver. Similar effects of electric charge have been observed for protein–dextran conjugates (3) and model macromolecules with the same molecular weight but different electric charges (4).

To investigate the mechanism underlying these phenomena, we examined the effect of electric charge on the hepatic uptake of macromolecules in an indicator dilution experiment using a single-pass rat liver perfusion system (5,6). In these studies, cationic macromolecules showed extensive hepatic uptake, an increased distribution volume, a marked degree of irreversible interaction, and a resultant large intrinsic clearance. Moreover, an *in vitro* association study performed with isolated rat hepatocytes (4,6) showed that cationic macromolecules were closely associated with the surface of hepatocyte membrane as a result of electrostatic forces. However, these findings concerned only the rapid phase of the hepatic uptake of cationic macromolecules, and slow processes, i.e., internalization, could not be detected in this experimental system. Accordingly, in this study we examined the hepatic disposition characteristics of model macromolecules with different electric charges in constant infusion experiments using a rat liver perfusion system, aiming to obtain detailed information on the hepatic uptake mechanism of such macromolecules.

MATERIALS AND METHODS

Animals

For the *in vivo* and liver perfusion experiments, male Wistar rats weighing, respectively, 240–250 and 190–210 g were used.

[1] Department of Basic Pharmaceutics, Faculty of Pharmaceutical Sciences, Kyoto University, Sakyo-ku, Kyoto 606, Japan.

[2] To whom correspondence should be addressed at Faculty of Pharmaceutical Sciences, Kyoto University, Sakyo-ku, Kyoto 606, Japan.

0724-8741/91/0400-0437$06.50/0

Chemicals

Dextran (T-70) was obtained from Pharmacia (Uppsala, Sweden). Type I collagenase and cytochalasin B were obtained from Sigma Chemical Co. (St Louis, Mo.). MMC was kindly supplied by Kyowa Hakko Kogyo (Tokyo), and [^{111}In]Cl_3 (74 MBq/ml) was kindly supplied by Nihon Mediphysics Co. (Takarazuka, Japan). Potassium [^{14}C]cyanide (30 MBq/mg) and γ-amino-[U-^{14}C]butyric acid (74 MBq/ml) were supplied by Amersham Japan (Tokyo) and New England Nuclear (Boston, Mass.), respectively. [Methoxy-^{14}C]inulin (185 MBq/g) was purchased from New England Nuclear (Boston, Mass.). All other chemicals were reagent-grade products that were obtained commercially.

Diethylaminoethyl–dextran (DEAE-Dex), carboxymethyl–dextran (CM-Dex), and cationized bovine serum albumin (Cat-BSA) were synthesized by the methods reported previously (7). Lac-BSA was synthesized by reductive amination with cyanoborohydride anion according to the method of Gray (8). MMC-Dcat (T-70) and MMC-Dan (T-70) were synthesized as reported previously (9,10). The physicochemical characteristics of these model macromolecules are summarized in Table I. The modified macromolecules had almost the same effective molecular size as the original dextran (T-70) and BSA on gel-filtration chromatography.

[Carboxyl-^{14}C]dextran (T-70) was prepared using potassium [^{14}C]cyanide according to the method of Isbell *et al.* (12) with a slight modification, and radiolabeled DEAE-Dex and CM-Dex were synthesized from this in the same manner as for the unlabeled molecules. Radiolabeled MMC-Dcat and MMC-Dan were synthesized as reported previously (10,13). Lac-BSA and Cat-BSA were labeled with ^{111}In using a bifunctional chelating agent, diethylenetriaminepentaacetic acid anhydride (Dojindo Labs, Kumamoto, Japan) according to the method of Hnatowich *et al.* (14).

In Vivo Disposition Experiment

Rats were anesthetized with pentobarbital and a saline solution of the radiolabeled macromolecule was injected into a femoral vein (50 mg/kg) after the bladder was cannulated with polyethylene tubing (i.d., 0.28 mm; o.d., 0.61 mm; Dural Plastics, Dural, Australia). The body temperature of the animals was kept at 37°C by a heat lamp during the experiments. Blood samples (0.2 ml) were withdrawn from the jugular vein over an 8-hr period and centrifuged at 3000 rpm for 2 min. At 8 hr after the injection, the liver was perfused with collagenase to isolate the liver cells just after the animal was killed. In addition, the heart, lung, spleen, intestine, muscle, and iliac lymph nodes were excised, rinsed with saline, weighed, and subjected to assay. For the liver, parenchymal cells (PC) were separated from nonparenchymal cells (NPC) by centrifugation (15). Cell viability was checked by the trypan blue dye exclusion method and was more than 90%.

Table I. Physicochemical Characteristics of the Model Macromolecules

Compound	MW (original)	pK_a[a]	Adsorption at pH 7.4 (%)[b] CM-Sephadex	Adsorption at pH 7.4 (%)[b] DEAE-Sephadex
Dextran	64,400	—	0	0
CM-Dex	64,400	3.2–3.3	0	99.6
DEAE-Dex	64,400	8.7–8.9	69.4	0
BSA	66,000	4.2–4.8	0	64.8
Lac-BSA	66,000	4.2–4.8	0	64.3
Cat-BSA	66,000	9.0–9.4	94.7	0
MMC-Dan	64,400	—	0	38.3
MMC-Dcat	64,400	—	97.1	0

[a] The pK_a values of the model macromolecules were measured by the acid–base titration method.

[b] Adsorption of the model macromolecules to CM-Sephadex and DEAE-Sephadex was measured by the batch method of Roos *et al.* (11).

Plasma concentration–time curves for the model macromolecules were fitted to the following biexponential equation by the nonlinear least-squares method (MULTI) (Yamaoka *et al.*) (16):

$$C(t) = A \cdot e^{-\alpha t} + B \cdot e^{-\beta t} \quad (1)$$

where $C(t)$ (% of dose/ml) represents the plasma concentration at time t. The area under the plasma concentration–time curve (AUC), the total-body clearance (CL_{total}), and the distribution volume in the steady state ($V_{d_{ss}}$) were calculated from these hybrid parameters.

Tissue distribution was evaluated by the tissue uptake rate index (CL_{in}) calculated in terms of clearance (μl/hr/g) as reported previously (1,7):

$$CL_{in} = T(t)/\int_0^t C(t)dt = T(t)/AUC_{0-t} \quad (2)$$

where $T(t)$ (% of dose/g) is the amount of a macromolecule in 1 g of tissue. This calculation was carried out by assuming linear uptake and negligible efflux (1,7). Then the total-organ clearance (CL_{org}) was expressed as follows:

$$CL_{org} = CL_{in} \cdot W \quad (3)$$

where W is the total weight of an organ. Urinary clearance (CL_{urine}) was calculated by Eq. (2) from the total urinary excretion. Cellular localization was evaluated by three indices: (i) the cellular uptake (μg/10^8 cells), (ii) the endocytic index (μl/hr/10^8 cells) calculated by dividing the uptake by the AUC for 8 hr, and (iii) the separate uptakes for PC and NPC (μg/g liver) calculated by multiplying the uptake by the number of each type of cells contained in 1 g of liver (1.25×10^8 cells/g liver for PC; 6.5×10^7 cells/g liver for NPC) (17).

Liver Perfusion Experiment

The operative procedure for *in situ* liver perfusion was modified from Moltimore's method (18). The liver was perfused at a flow rate of 13 ml/min using a single-pass mode. The perfusion medium was Krebs–Ringer bicarbonate buffer with 10 m*M* glucose, which was oxygenated with 95% O_2–5% CO_2 to pH 7.4 at 37°C and contained neither erythrocytes nor albumin.

After a stabilization period of 30 min, model macromolecules dissolved in the perfusate (10 or 50 μg/ml) were infused for 1 hr. In the endocytosis inhibition study, colchicine

(20 μ*M*) or cytochalasin B (2 μg/ml) was also added to the perfusate. The venous outflow of the perfusate and bile samples were collected into tubes at appropriate intervals. At the completion of infusion, perfusate without macromolecules was infused for 5 min to wash out the remaining compounds from the intravascular compartment and spaces of Disse. Then the liver was perfused with collagenase and the PC and NPC fractions were obtained by differential centrifugation. Cell viability was checked by the trypan blue dye exclusion method. In the acid-wash experiment, the perfusate was replaced for 10 min with ice-cold acidified buffer (pH 3) (19) at the completion of infusion, and the dissociated radioactivity was detected.

From the outflow curves, the E_{ss} and the hepatic clearance of the model macromolecules (CL_h) were calculated as follows:

$$E_{ss} = (C_{in} - C_{out})/C_{in} \quad (4)$$

$$CL_h = E_{ss} \cdot Q \quad (5)$$

where C_{in} and C_{out} are the concentrations of model macromolecules in the perfusate before and after passing through the liver under steady-state conditions, and Q is the perfusion rate.

Determination of Radioactivity

The determination of ^{14}C radioactivity was carried out by liquid scintillation counting (Model LSC 5000C, Beckman). One milliliter of an aqueous sample was added to a vial with 5 ml of the scintillation medium (Clear-sol I, Nacalai Tesque, Kyoto, Japan). The plasma, urine, and cell suspensions were placed into counting vials with 0.7 ml of Soluene-350 (Packard Instrument, USA). After incubation at 45°C for 10 hr, 5 ml of scintillation medium was added.

The ^{111}In radioactivity was counted using a well-type NaI scintillation counter without any special procedures.

RESULTS

Plasma Elimination and Tissue Distribution of Macromolecules

The plasma concentrations of the radiolabeled model macromolecules were determined for 8 hr after intravenous injection (Fig. 1). Each macromolecule showed biphasic elimination, and the pharmacokinetic parameters calculated on the basis of the two-compartment model are summarized in Table II. Anionic macromolecules (^{14}C-CM-Dex and ^{14}C-MMC-Dan) had a small total-body clearance, while cationic macromolecules (^{14}C-DEAE-Dex, ^{111}In-Cat-BSA, and ^{14}C-MMC-Dcat) showed a large clearance and the neutral macromolecule (^{14}C-dextran) had an intermediate value. The distribution volumes of the anionic macromolecules were roughly equal to the plasma volume of the rats (ca. 10 ml) (20), but those of ^{111}In-Cat-BSA and ^{14}C-MMC-Dcat were much larger. The tissue uptake index was also affected by the electric charge (Table II) and cationic macromolecules were markedly accumulated in the liver, spleen, and kidneys, with the liver being the major site of accumulation. As for the urinary excretion, the dextran derivatives generally had a larger urinary clearance than the albumin derivatives.

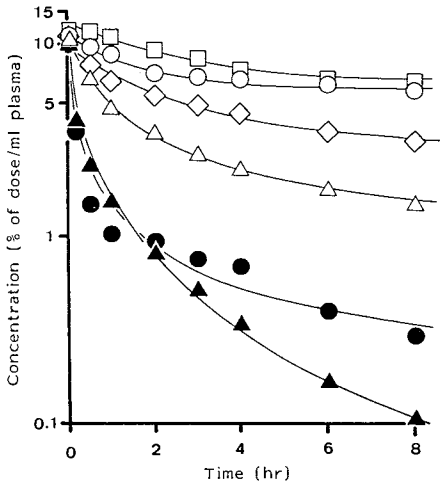

Fig. 1. Plasma concentrations of the radiolabeled model macromolecules after intravenous injection into rats. Results are expressed as the mean of three experiments. ◇, ^{14}C-Dextran; □, ^{14}C-CM-Dex; △, ^{14}C-DEAE-Dex; ▲, ^{111}In-Cat-BSA; ○, ^{14}C-MMC-Dan; ●, ^{14}C-MMC-Dcat.

Cellular Localization of Macromolecules in the Liver

Table III shows the distribution of macromolecules between PC and NPC at 8 hr after intravenous injection. The uptake of both ^{111}In-Cat-BSA and ^{14}C-MMC-Dcat was about 10 times as great as that of the anionic and neutral macromolecules in both cell types. The differences were even more marked in the endocytic index values. The uptake calculated for each cell type suggested that the PC were more involved in the uptake of cationic macromolecules, but the difference was not so much as in the case of Lac-BSA, which is known to be taken up by PC by receptor-mediated endocytosis (21).

Hepatic Uptake During Constant Infusion of Macromolecules

Figure 2 illustrates the hepatic recovery ratio (C_{out}/C_{in})–time profiles of various macromolecules in the rat liver perfusion system. In this case, the inflow concentration of 10 μg/ml approximately corresponds to the concentration of 0.1% of the dose per ml in the plasma elimination curve (Fig. 1). The total dose during 60 min of infusion (7.8 mg) was 60% of that given in the *in vivo* experiment. Anionic and neutral macromolecules (^{14}C-CM-Dex, ^{14}C-MMC-Dan, and ^{14}C-dextran) showed similar profiles, reached steady-state conditions within 5 min, and had a recovery ratio approaching 1.0. In contrast, the hepatic recovery ratio of ^{111}In-Cat-BSA and ^{14}C-MMC-Dcat gradually increased with time up to 40 min after the start of perfusion. In addition, a lag time (delayed appearance in the outflow) of about 5 min was observed for these cationic macromolecules. In all cases, the recovery ratio at 60 min was taken as the steady-state value and was used to calculate the clearance. Table IV summarizes the results together with the data for ^{14}C-inulin, which was used as an extracellular marker. The recovery values calculated from the radioactivity in liver tissue and bile samples are also listed in Table IV. Hepatic uptake of ^{111}In-Cat-BSA and ^{14}C-MMC-Dcat was extremely large, while an-

Table II. Pharmacokinetic Parameters for the Model Macromolecules after Intravenous Injection into Rats[a]

Compound	AUC (% dose · hr/ml)	$V_{d_{ss}}$ (ml)	CL_{total} (μl/hr)	CL_{urine} (μl/hr)	CL_{liver} (μl/hr)	Tissue uptake rate index (μl/hr/g)		
						Liver[b]	Spleen	Kidney
^{14}C-Dextran	65.23	14.2	1,532	677	53	6.2	9.6	9.9
^{14}C-CM-Dex	112.14	8.3	890	283	15	1.8	4.3	3.3
^{14}C-DEAE-Dex	33.43	19.1	3,003	1,844	609	67.7	44.9	66.9
^{111}In-Cat-BSA	5.67	38.0	17,640	296	14,958	2,167.8	1,271.5	820.9
^{14}C-MMC-Dan	93.28	10.5	1,074	275	37	4.1	6.1	4.0
^{14}C-MMC-Dcat	7.30	66.8	13,693	1,199	8,606	765.0	807.2	770.4

[a] Results are expressed as the mean of three experiments.
[b] The tissue uptake rate index for the liver was calculated from the uptake by isolated PC and NPC using the total cell numbers reported in the literature (17).

ionic and neutral macromolecules showed little uptake. ^{14}C-MMC-Dcat showed the largest biliary excretion among the model macromolecules. With acid-wash treatment, 14.5 and 3.6% of the ^{111}In-Cat-BSA and ^{14}C-MMC-Dcat extracted by the liver were respectively stripped off under control conditions (10 μg/ml, 37°C).

Cellular Localization of Macromolecules After Constant Infusion

The cellular distribution of radiolabeled macromolecules between PC and NPC after constant infusion for 60 min is also summarized in Table III. A significant interaction of the cationic macromolecules with PC was suggested by the results. PC/NPC ratios for the cationic macromolecules were basically similar to those obtained in the *in vivo* study. The total uptake calculated from the uptake for each type of cell was about 85% of that estimated from integration of the outflow curve, suggesting the validity of these results.

Effect of Dose, Temperature, and Treatment with Colchicine and Cytochalasin B on Hepatic Uptake During Constant Infusion

The hepatic recovery ratio–time profiles of ^{111}In-Cat-BSA and ^{14}C-MMC-Dcat at inflow concentrations of 10 and 50 μg/ml are compared in Figs. 3 and 4, respectively. At steady state, the hepatic clearance of both compounds was markedly decreased (Table V) and the time required to attain steady state was shortened by high inflow concentrations and low temperature (15°C). Figures 3 and 4 also show the effects of the administration of colchicine and cytochalasin B on the hepatic recovery ratio–time profiles of ^{111}In-Cat-BSA and ^{14}C-MMC-Dcat, respectively. Colchicine treatment decreased the hepatic clearance of ^{111}In-Cat-BSA and ^{14}C-MMC-Dcat to 19 and 65% of the control level, respectively, while cytochalasin B decreased clearance to 28 and 50% of control level. Furthermore, the time required to attain steady state was significantly shortened by the addition of these compounds.

Table III. Distribution of the Model Macromolecules in Rat Liver Parenchymal (PC) and Nonparenchymal Cells (NPC) in the *in Vivo* Experiment at 8 hr and the Constant-Infusion Experiment at 1 hr

Compound	Cell type	*In vivo*			Constant infusion	
		Uptake (μg/10^8 cells)	Endocytic index (μl/hr/10^8 cells)	Uptake amount (μg/g liver)	Uptake (μg/10^8 cells)	Uptake amount (μg/g liver)
^{14}C-Dextran	PC	33.4 ± 7.4	3.9	41.6	0	0
	NPC	18.6 ± 3.3	2.2	12.1	0	0
^{14}C-CM-Dex	PC	12.9 ± 1.5	0.9	16.1	0	0
	NPC	14.1 ± 1.9	1.0	9.1	0	0
^{14}C-DEAE-Dex	PC	65.4 ± 14.3	15.2	81.8	16.7 ± 5.6	20.8
	NPC	20.6 ± 7.5	4.7	13.5	6.7 ± 0.6	4.4
^{111}In-Lac-BSA	PC	938.8 ± 60.9	382.4	1173.5	57.7 ± 5.4	72.2
	NPC	66.6 ± 13.4	28.2	43.3	4.8 ± 1.3	3.1
^{111}In-Cat-BSA	PC	1034.4 ± 118.1	1380.2	1292.9	244.6 ± 36.5	305.7
	NPC	375.6 ± 101.9	526.1	243.4	62.4 ± 7.3	40.6
^{14}C-MMC-Dan[b]	PC	25.5 ± 5.9	3.1	31.8	0	0
	NPC	24.9 ± 6.0	2.6	16.2	0	0
^{14}C-MMC-Dcat[b]	PC	321.0 ± 67.8	440.3	401.3	248.4 ± 19.8	310.5
	NPC	230.0 ± 45.5	336.2	149.9	125.1 ± 28.4	81.3

[a] Results are expressed as the mean ± SD of at least three experiments.
[b] Results were reported previously (6).

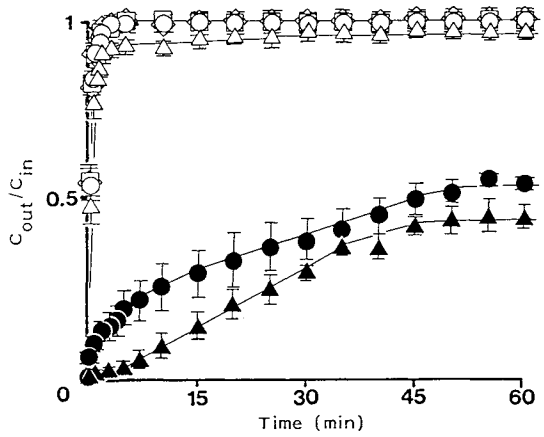

Fig. 2. Hepatic recovery ratio (C_{out}/C_{in})–time profiles for the model macromolecules in the isolated rat liver perfusion system (inflow concentration, 10 μg/ml). Results are expressed as the mean ± SD of at least three experiments. ◇, ^{14}C-Dextran; □, ^{14}C-CM-Dex; △, ^{14}C-DEAE-Dex; ▲, ^{111}In-Cat-BSA; ○, ^{14}C-MMC-Dan; ●, ^{14}C-MMC-Dcat.

DISCUSSION

In the *in vivo* experiment, the calculated endocytic indices for anionic and neutral macromolecules were broadly similar to those reported for polyvinylpyrolidone, which is taken up by the liver through fluid-phase endocytosis (3.11 and 2.60 μl/hr/10^8 cells for PC and NPC, respectively) (22). Consequently, these macromolecules are also considered to be taken up by fluid-phase endocytosis. The E_{ss} values calculated from these endocytic indices in the constant infusion experiment were less than 1%, a level which could not be experimentally detected (Table IV).

For the cationic macromolecules, hepatic uptake and subsequent degradation were the main routes of elimination, since the contribution of hepatic clearance to total-body clearance was very high (Table II). This was confirmed not only by the *in vivo* experiment but also by experiments using the perfusion system without erythrocytes and albumin. Blood components were thus suggested to have only a minor effect on the handling of these macromolecules.

Cationic macromolecules were taken up by both PC and NPC in proportion to their surface area ratios in both the *in vivo* and the liver perfusion experiments. PC occupy 73% of the surface area of the liver plasma membrane (17), a value that is consistent with the present results (Table III). Thus, the cationic macromolecules appeared to be localized nonspecifically in both cell types. In the present study, we focused on the interaction of the macromolecules with PC. In contrast, Lac-BSA has been reported to be taken up by PC having a receptor for terminal galactose (21), and the present liver preparation maintained this physiological function (Table III).

Cationic macromolecules have been previously found to associate with the surface of liver cells in conformity to Langmuir's adsorption isotherm (4,6). Macromolecules on the cell surface may then be internalized into the cells with the rate constant, k_{int}. However, since the adsorption to the cell surface is far greater than the rate of internalization, no significant difference was observed between incubation at 4°C and that at 37°C in the association of cationic macromolecules with liver cells. Consequently, to detect the internalization process, a constant infusion system was considered to be advantageous over association time-course determinations. Under steady-state conditions in the constant-infusion experiment, the elimination rate of macromolecules from the perfusate, i.e., $(C_{in} - C_{out}) \cdot Q$, equals the internalization rate, which is expressed as a product of X (association amount) at $C = C_{out,ss}$ and k_{int}.

Figure 5A shows the relationship between the X values for the cationic macromolecules calculated from the binding parameters obtained in the *in vitro* association experiment (4) and the steady-state uptake rates determined in the constant infusion experiment. Calculation of X values based on acid-washing data was not performed, because only partial removal (ca. 10%) of cationic macromolecules was observed in the *in vitro* association experiment even at 4°C (4). The linear relationship shown in Fig. 5A ($r = 0.998$) suggests that the internalization rate constants were similar for these compounds, and the saturable uptake shown in Table V is also accounted for by these results.

The slope of this relationship might correspond to the product of k_{int} and the ratio between the *in vivo* total liver cell surface area and that constructed from the *in vitro* data. The k_{int} value for cationic macromolecules has been calculated to be 0.015 min^{-1} on the basis of sinusoidal hepatocyte surface area (17), a value that was much smaller than those

Table IV. Hepatic Clearance and Radioactivity Recoveries for the Model Macromolecules in the Constant-Infusion Experiment[a]

Compound	Outflow		Amount recovery	
	E_{ss} (%)	CL_h (μl/min)	Liver (μg)	Bile (μg)
^{14}C-Inulin	0	0	5.6 ± 1.6	0.19 ± 0.09
^{14}C-Dextran	0	0	38.4 ± 4.0	0.68 ± 0.29
^{14}C-CM-Dex	0	0	67.2 ± 16.1	0.46 ± 0.17
^{14}C-DEAE-Dex	2.8 ± 0.2	360 ± 30	478.1 ± 52.6	0.69 ± 0.23
^{111}In-Cat-BSA	53.6 ± 2.9	6841 ± 392	3924.1 ± 129.6	0.73 ± 0.11
^{14}C-MMC-Dan	0	0	16.8 ± 0.8	1.68 ± 0.56
^{14}C-MMC-Dcat	45.6 ± 2.7	6003 ± 423	5578.4 ± 314.4	47.49 ± 16.67

[a] Results are expressed as the mean ± SD of at least three experiments.

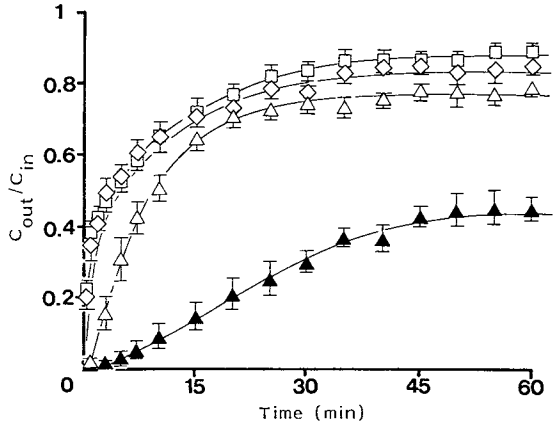

Fig. 3. Hepatic recovery ratio (C_{out}/C_{in})–time profiles for ^{111}In-Cat-BSA under various experimental conditions in the isolated rat liver perfusion system. Results are expressed as the mean ± SD of at least three experiments. ▲, Control (10 μg/ml); △, high dose (50 μg/ml); □, colchicine treatment; ◇, cytochalasin B treatment.

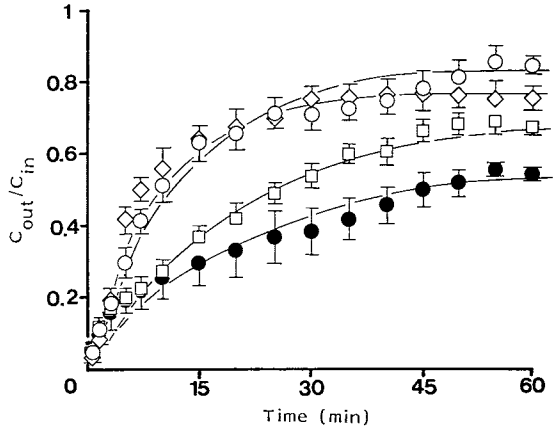

Fig. 4. Hepatic recovery ratio (C_{out}/C_{in})–time profiles for ^{14}C-MMC-Dcat under various experimental conditions in the isolated rat liver perfusion systems. Results are expressed as the mean ± SD of at least three experiments. ●, Control (10 μg/ml); ○, high dose (50 μg/ml); □, colchicine treatment; ◇, cytochalasin B treatment.

reported for ligands such as asialoorosomucoid (0.48 min^{-1}) (23) and epidermal growth factor (0.33 min^{-1}) (19), which are internalized by a receptor-mediated mechanism.

The relationship between the amount of cationic macromolecules taken up via irreversible interactions shown in a previous indicator dilution experiment (4) and the steady-state uptake rate during constant infusion is also plotted in Fig. 5B, and again, a linear relation is observed.

During the constant infusion of ^{111}In-Cat-BSA (C_{in}; 10 μg/ml), a lag time of about 5 min was observed before its appearance in the outflow. This result might reflect rapid association and slow dissociation, which was detected as irreversible association in the previous indicator dilution experiment (4).

In the organ disposition model discussed above, the time required to attain steady-state conditions is prolonged as X_∞ or the k_{int} value increased. The effect of changes of the binding affinity of the macromolecules to the cell surface, i.e., changes of K (binding constant), is more complicated. In the present case, the prolongation of the time required to achieve steady state might correspond to an increase in binding under steady-state conditions, because k_{int} was similar among the cationic macromolecules.

Colchicine and cytochalasin B are known to inhibit pinocytic and phagocytic endocytosis, respectively (24–27). Colchicine depolymerizes cytoplasmic microtubules and causes a reduction in the basal pinocytic rate, whereas cytochalasin B impairs actin gelatin and microfilament function to inhibit phagocytosis. Both colchicine and cytochalasin B inhibited the hepatic uptake of ^{111}In-Cat-BSA and ^{14}C-MMC-Dcat. If the hepatocyte binding affinity and/or capacity for ^{111}In-Cat-BSA and ^{14}C-MMC-Dcat to interact with hepatocytes were unaffected by the coadministration of these two compounds, the reduction of apparent uptake rate

Table V. Hepatic Clearance and Radioactivity Recoveries for ^{14}C-MMC-Dcat and ^{111}In-Cat-BSA Under Various Experimental Conditions in the Constant-Infusion Experiment[a]

Condition	C_{in} (μg/ml)	Outflow		Amount recovery	
		E_{ss} (%)	CL_h (μl/min)	Liver (μg)	Bile (μg)
^{111}In-Cat-BSA					
Control	10	53.6 ± 2.9	6841 ± 392	3924.1 ± 129.6	0.73 ± 0.11
Colchicine[b]	10	10.5 ± 0.1	1314 ± 145	867.2 ± 81.6	0.50 ± 0.12
Cytochalasin B[c]	10	15.1 ± 0.1	1896 ± 152	1284.0 ± 129.5	0.64 ± 0.22
High dose	50	23.2 ± 1.2	3094 ± 213	5751.1 ± 416.5	0.94 ± 0.01
15°C	50	11.4 ± 1.8	1451 ± 230	4334.4 ± 211.3	0.01 ± 0.01
^{14}C-MMC-Dcat					
Control	10	45.6 ± 2.7	6003 ± 423	5578.4 ± 314.4	47.49 ± 16.67
Colchicine[b]	10	32.5 ± 3.6	3912 ± 421	4882.4 ± 455.2	9.57 ± 0.10
Cytochalasin B[c]	10	24.4 ± 0.1	3014 ± 123	3852.0 ± 155.2	0.97 ± 0.35
High dose	50	19.4 ± 2.0	2326 ± 274	14724.8 ± 405.6	255.73 ± 9.40
15°C	50	6.9 ± 1.4	836 ± 156	12968.2 ± 506.3	0.04 ± 0.01

[a] Results are expressed as the mean ± SD of at least three experiments.
[b] 20 μ*M*.
[c] 2 μg/ml.

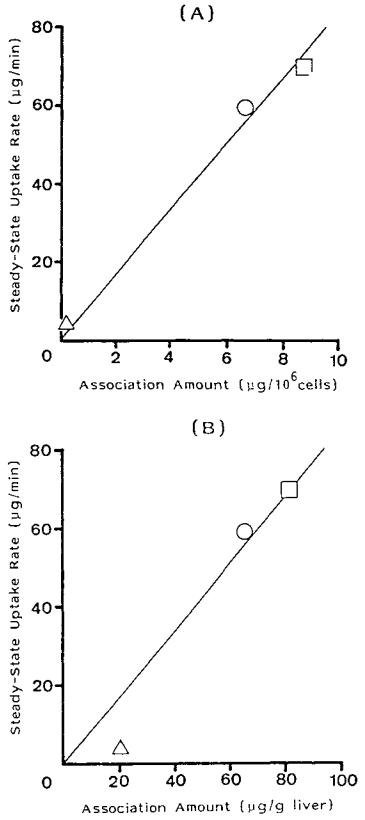

Fig. 5. Relationships between the steady-state hepatic uptake rate and the association amount of cationic macromolecules with hepatocytes in the *in vitro* association experiment (A) and indicator dilution experiment (B) (4). △, ^{14}C-DEAE-Dex; □, ^{111}In-Cat-BSA; ○, ^{14}C-MMC-Dcat.

at steady state could have resulted from a decrease in the internalization rate constant (k_{int}). Since both colchicine and cytochalasin B inhibited the uptake of ^{111}In-Cat-BSA and ^{14}C-MMC-Dcat, microfilaments as well as microtubules might be involved in the hepatic uptake of cationic macromolecules.

We also observed that the E_{ss} for ^{111}In-Cat-BSA and ^{14}C-MMC-Dcat significantly decreased during low-temperature perfusion at 15°C, with steady-state conditions being attained at 20 min after the start of perfusion (E_{ss} values of 5–10%). This finding argues for the existence of an internalization process for cationic macromolecules.

After internalization, macromolecules might be exposed to lysosomal enzymes. Dextran is fairly resistant to such enzymes, but the protein derivatives we used are likely to have been degraded, and subsequently the ^{111}In label would be transported with iron-binding protein (28). The biliary recovery of ^{14}C-MMC-Dcat was about 100 times greater than that of ^{111}In-Cat-BSA in the constant-infusion experiment (Table IV). Differences in the mode of degradation of these macromolecules could contribute at least partly to this discrepancy.

In conclusion, the hepatic uptake of cationic macromolecules occurred by their nonspecific adsorption to the surface of hepatocytes by electrostatic forces, with a subsequent putative internalization by adsorptive endocytosis. The contribution of PC to this binding was predominant. Such information on the hepatic disposition of macromolecules should be useful in the development of macromolecular prodrugs or protein carrier systems.

REFERENCES

1. Y. Takakura, A. Takagi, M. Hashida, and H. Sezaki. Disposition and tumor localization of mitomycin C-dextran conjugates in mice. *Pharm. Res.* 4:293–300 (1987).
2. Y. Takakura, R. Atsumi, M. Hashida, and H. Sezaki. Development of a novel polymeric prodrug of mitomycin C, mitomycin C-dextran conjugate with anionic charge. II. Disposition and pharmacokinetics following intravenous and intramuscular administration. *Int. J. Pharm.* 37:145–154 (1987).
3. T. Fujita, Y. Yasuda, Y. Takakura, M. Hashida, and H. Sezaki. Alteration of biopharmaceutical properties of drugs by their conjugation with water-soluble macromolecules: Uricase-dextran conjugate. *J. Control. Release* 11:149–156 (1990).
4. K. Nishida, C. Tonegawa, S. Nakane, Y. Takakura, M. Hashida, and H. Sezaki. Effect of electric charge on the hepatic uptake of macromolecules in the rat liver. *Int. J. Pharm.*, 65:7–17 (1990).
5. K. Sato, K. Itakura, K. Nishida, Y. Takakura, M. Hashida, and H. Sezaki. Disposition of a polymeric prodrug of mitomycin C-dextran conjugate, in the perfused rat liver. *J. Pharm. Sci.* 78:11–16 (1989).
6. S. Nakane, S. Matsumoto, Y. Takakura, M. Hashida, and H. Sezaki. The accumulation mechanism of cationic mitomycin C-dextran conjugates in the liver: In-vivo cellular localization and in-vitro interaction with hepatocytes. *J. Pharm. Pharmacol.* 40:1–6 (1988).
7. Y. Takakura, T. Fujita, M. Hashida, and H. Sezaki. Disposition characteristics of macromolecules in tumor-bearing mice. *Pharm. Res.* 7:339–346 (1990).
8. G. R. Gray. The direct coupling of oligosaccharides to proteins and derivatized gels. *Arch. Biochem. Biophys.* 163:426–428 (1974).
9. T. Kojima, M. Hashida, S. Muranishi, and H. Sezaki. Mitomycin C-dextran conjugate: A novel high molecular weight prodrug of mitomycin C. *J. Pharm. Pharmacol.* 32:30–34 (1980).
10. Y. Takakura, M. Kitajima, S. Matsumoto, M. Hashida, and H. Sezaki. Development of a novel polymeric prodrug of mitomycin C, mitomycin C-dextran conjugate with anionic charge. I. Physicochemical characteristics and in vivo and in vitro antitumor activities. *Int. J. Pharm.* 37:135–143 (1987).
11. C. F. Roos, S. Matsumoto, Y. Takakura, M. Hashida, and H. Sezaki. Physicochemical and antitumor characteristics of some polyamino acid prodrugs of mitomycin C. *Int. J. Pharm.* 22:75–87 (1984).
12. H. S. Isbell, H. L. Frush, and J. D. Moyer. ^{14}C and ^{3}H for the study and characterization of cellulose and other polysaccharides. *Tech. Assoc. Pulp Paper Ind.* 40:739–742 (1957).
13. M. Hashida, A. Kato, Y. Takakura, and H. Sezaki. Disposition and pharmacokinetics of a polymeric prodrug of mitomycin C, mitomycin C-dextran conjugate, in the rat. *Drug Metab. Dispos.* 12:492–499 (1984).
14. D. J. Hnatowich, W. W. Layne, and R. L. Childs. The preparation and labeling of DTPA-coupled albumin. *Int. J. Appl. Radiat. Isot.* 33:327–332 (1982).
15. S. Horiuchi, K. Takata, and Y. Morino. Characterization of a membrane-associated liver cells that binds formaldehyde-treated serum albumin. *J. Biol. Chem.* 260:475–481 (1985).
16. K. Yamaoka, T. Tanigawara, T. Nakagawa, and T. Uno. A pharmacokinetic analysis program (MULTI) for microcomputer. *J. Pharmacobio-Dyn.* 4:879–885 (1981).
17. R. Blomhoff, H. K. Blomhoff, H. Tolleshaug, T. B. Christensen, and T. Berg. Uptake and degradation of bovine testes β-galactosidase by parenchymal and nonparenchymal rat liver cells. *Int. J. Biochem.* 17:1321–1328 (1985).

18. G. E. Mortimore, F. Tietze, and D. Stetten. Metabolism of insulin-^{131}I. Studies in isolated, perfused rat liver and hindlimb preparations. *Diabetes* 8:307–314 (1959).
19. H. Sato, Y. Sugiyama, Y. Sawada, T. Iga, T. Fuwa, and M. Hanano. Internalization of EGF in perfused rat liver is independent of the degree of receptor occupancy. *Am. J. Physiol.* 258:G682–G689 (1990).
20. L. E. Gerlowski and R. K. Jain. Physiologically based pharmacokinetic modeling: Principles and applications. *J. Pharm. Sci.* 72:1103–1126 (1983).
21. G. Ashwell and J. Harford G. Carbohydrate-specific receptors of the liver. *Annu. Rev. Biochem.* 51:531–546 (1982).
22. J. Munniksma, M. Noteborn, T. Kooistra, S. Stienstra, J. M. W. Bouma, M. Gruber, A. Brower, D. P. Praaning-Van Dalen, and D. L. Knook. Fluid endocytosis by rat liver and spleen: Experiments with ^{125}I-labeled poly(vinylpyrrolidone) in vivo. *Biochem. J.* 192:613–621 (1980).
23. A. L. Schwartz, S. E. Fridovich, and H. F. Lodish. Kinetics of internalization and recycling of the asialoglycoprotein receptor in a hepatoma cell line. *J. Biol. Chem.* 257:4230–4237 (1982).
24. A. N. Bhisey and J. J. Freed. Altered movement of endosomes in colchicine-treated cultured macrophages. *Exp. Cell Res.* 64:430–438 (1971).
25. E. L. Pesanti and S. G. Axline. Phagolysosome formation in normal and colchicine-treated macrophages. *J. Exp. Med.* 142:903–913 (1975).
26. G. G. Klaus. Cytochalasin B: Dissociation of pinocytosis and phagocytosis by peritoneal macrophages. *Exp. Cell Res.* 79:73–78 (1973).
27. J. H. Hartwig and T. P. Stossel. Interactions of actin, myosin, and actin-binding protein of rabbit pulmonary macrophages. III. Effects of cytochalasin B. *J. Cell Biol.* 71:295–303 (1976).
28. B. A. Brown, R. D. Comeau, P. L. Jones, F. A. Liberatore, W. P. Neacy, H. Sands, and B. M. Gallagher. Pharmacokinetics of the monoclonal antibody B72.3 and its fragments labeled with either ^{125}I or ^{111}In. *Cancer Res.* 47:1149–1154 (1987).